ARACOR

LEVEL 12

AD A106357

'ETAL-SEMICONDUCTOR REACTION PHENOMENA AND MICROSTRUCTURAL
TIGATIONS OF LASER INDUCED REGROWTH OF SILICON ON INSULATORS

ANNUAL PROGRESS REPORT

JANUARY 1981

DTIC
ELECTE
OCT 3 0 1981

H

PREPARED FOR:

U.S. ARMY RESEARCH OFFICE
CONTRACT NO. DAAG29-79-C-0014

DTIC FILE COPY

81 1 26 078

18) A H A   (19) 25919.5-MS

SECURITY CLASSIFICATION OF THIS PAGE (When Data Entered)

REPORT DOCUMENTATION PAGE		READ INSTRUCTIONS BEFORE COMPLETING FORM
1 REPORT NUMBER TR-81-37-1	2 GOVT ACCESSION NO	3 RECIPIENT'S CATALOG NUMBER
4 TITLE (and Subtitle) Metal-Semiconductor Reaction Phenomena and Microstructural Investigations of Laser-Induced Regrowth of Silicon on Insulators		5 TYPE OF REPORT & PERIOD COVERED Annual Report January, 1980 to December, 1980
		6 PERFORMING ORG. REPORT NUMBER
7 AUTHOR(s) T.J. Magee, C. Leung, R. Ormond and R.A. Armistead		8 CONTRACT OR GRANT NUMBER(s) DAAG29-79-C-0014
9 PERFORMING ORGANIZATION NAME AND ADDRESS Advanced Research and Applications Corporation 1223 East Arques Avenue Sunnyvlae, California 94086		10 PROGRAM ELEMENT, PROJECT, TASK AREA & WORK UNIT NUMBERS 351
11 CONTROLLING OFFICE NAME AND ADDRESS U.S. Army Research Office Post Office Box 12111 Research Triangle Park, NC 27709		12 REPORT DATE January, 1981
		13 NO. OF PAGES 22
14 MONITORING AGENCY NAME & ADDRESS (if diff. from Controlling Office) ARAZOR-TR-81-37-1		15 SECURITY CLASS (of this report) UNCLASSIFIED
		15a DECLASSIFICATION/DOWNGRADING SCHEDULE NA

16 DISTRIBUTION STATEMENT (of this report)

Approved for public release; distribution unlimited.

17 DISTRIBUTION STATEMENT (of the abstract entered in Block 20 if different from report)

NA

18 SUPPLEMENTARY NOTES

The findings in this report are not to be construed as an official Department of the Army position, unless so designated by other authorized documents.

19 KEY WORDS (Continue on reverse side if necessary and identify by block number)

Epitaxial Layers	Electrical Contacts	Thin Films
Silicon-on-Sapphire	Diffusion	
Laser Annealing	Transmission Electron Microscopy	
Liquid Phase Epitaxy	Rutherford Backscattering	
Gallium Arsenide	Microstructural Defects	

20 ABSTRACT (Continue on reverse side if necessary and identify by block number)

The defect structure in CVD Si layers on sapphire were investigated before and after scanning laser annealing. Prior to laser annealing, the films were characterized by the presence of stacking faults, twinning zones and dislocation lines producing large regions of high disorder. Subsequent to laser annealing under conditions to produce total melting of the Si layers it was shown that liquid phase epitaxial regrowth occured resulting in regions of defect-free Si and a total absence of twinning regions. Correlated Rutherford backscattering, channeling and transmission elecron microscopic analyses showed a dramatic

DD FORM 1473 EDITION OF 1 NOV 65 IS OBSOLETE

improvement in crystalline perfection relative to the results obtained from films grown by any other technique on sapphire substrates.

In separate collaborative experiments with Stanford University, it was also shown that scanning cw laser irradiation could be used to produce diffusion and activation of Sn from a spin-on SnO_2/SiO_2 source. The formation of a Sn_3As_2 alloy has been shown to be related to the observed n^+ activity.
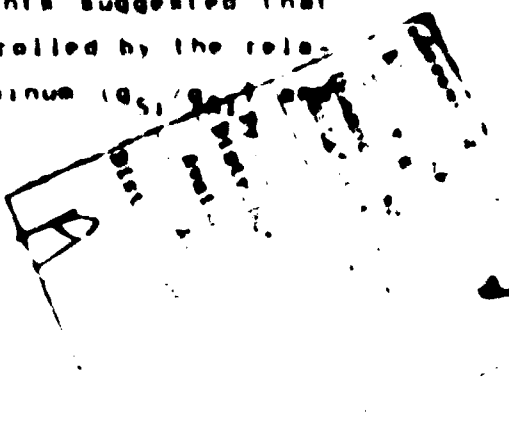
INTRODUCTION

Reactions between metal films and single or poly-crystalline silicon substrates have received considerable attention over the past decades because of the relevancy to integrated circuit fabrication and design. The aluminum-silicon (Al/Si) system has been widely investigated in relation to its use in contact structures, as a diffusion source and in silicon-gate MOS technology.

In an early phase of this program, it was shown that interactions between a polycrystalline Al film and single-crystal Si were controlled, in part, by grain boundary kinetics and the presence of microstructural defects within individual Al grains. Interdiffusion between the Al and Si was initiated at Al grain boundary sites and within defective Al groups producing Si-saturated Al films and localized Al-doped regions within the Si substrate. Upon cooling, lateral motion of Si to grain boundaries occurred, accompanied by a solid-phase regrowth of silicon hillocks on the single-crystal substrate.

Subsequent experiments conducted on the Al(poly)/Si(poly)/SiO$_2$/Si (crystal) system showed that after heating at 500°C, Si was transported through the Al film to form a continuous Si film at the surface. Growth was initiated at grain boundaries of the Al film and individual growth islands expanded by lateral accretion, yielding a coalesced continuous poly-Si film at the surface.

The data obtained in these experiments suggested that the solid-phase regrowth process was controlled by the relative grain sizes of the silicon and aluminum (q_{Si},

relative thickness (t_{Si}/t_{Al}). Research in the first phase of the current program tended to verify these assumptions, confirming that as $g_{Si}/q_{Al} \rightarrow \infty$ (for $t_{Si}/t_{Al} \simeq 1$,), solid-phase interchange of layer positions was relatively inhibited.

To extend these results, we conducted a series of experiments on regrowth of Si on sapphire in the Si(amorphous)/Al(poly)/Al$_2$O$_3$(crystal) system. The primary objective was to determine if the solid-phase regrowth process could be correlated with a classical island growth/coalescence model within a known system, where island coalescence is the dominant mechanism in liquid-phase epitaxial growth.

These experiments demonstrated that solid-phase regrowth of Si on sapphire can be obtained using Al as the transport medium. The results show that the Si is transported through the Al film to form nucleation sites on the sapphire substrate. These sites expand laterally by mass accretion and coalescence to form islands continuous with the underlying substrate. During the final growth sequence, the coalescence of larger island structures is characterized by the presence of twinning zones and defects at the juncture region. Direct observation by TEM/SEM at various stages of annealing confirm that the (structural) regrowth sequence is similar to that observed during conventional liquid-phase epitaxy growth of Si on sapphire. However, one problem with standard LPE SOS structures is the relatively-high density of twins, stacking faults and dislocation lines in the epitaxial silicon. The regrown silicon layers prepared in these experiments exhibited comparable defect densities and distribution of defects within the Si film.

For electronic device fabrication, it would be very valuable to develop techniques for the growth of epitaxial

silicon on sapphire (or another suitable dielectric subs-
trate) with a low defect concentration. The potential
importance of SOS structures is suggested by the fact that
a number of organizations proposed the use of SOS struc-
tures to satisfy the technical requirements of the current
DoD-funded Very-High-Speed Integrated Circuits (VHSIC)
Program.

However, in spite of over two decades of research on
the growth and control of silicon thin films grown epitax-
ially on single-crystal sapphire (Al_2O_3), difficult problems
remain. Of particular concern is the high level of de-
fects present within the epitaxial Si layer, both at the
interface and within the bulk of the film. These defect
concentrations influence metal-semiconductor reactions in
the contact and interconnection regions and prove to be a
severe restrictive factor on the fabrication of devices.
The measurable reduction in electron mobility in the pre-
sence of these defect strucutures places limits on the
speed or switching capability of SOS-based devices.

For these reasons, in this reporting period we focused
our effort on developing a technique for producing SOS
structures with substantially reduced defect concentrations.

Recently, a number of investigators have suggested
that the quality of silicon layers on sapphire (or, per-
haps, some other suitable dielectric substrate) can be
improved by pulsed laser irradiation to induce regrowth
of the deposited layers by a liquid-phase epitaxial mecha-
nism. Preliminary experiments have also shown that scan-
ning CW argon laser annealing can also produce regrowth
of the deposited layers, with an apparent reduction in
defect density. In all cases, there have been no detailed

investigations of the recrystallization of the Si layers
on the microstructural perfection of reordered layers after
laser annealing.

Thus, we initiated experiments in collaboration with
I. Golecki of Rockwell Labs toward a detailed study of
microstructural defects within both control and laser-
annealed SOS structures in both the solid-phase regrowth
(SPEG) and liquid-phase regrowth (LPE) modes. Correla-
ted data from transmission electron microscopy/diffraction
(TEM/TED), scanning electron microscopy (SEM), Auger elec-
tron spectroscopy (AES), secondary ion mass spectrometry
(SIMS), Rutherford back scattering (RBS), and Hall effect
measurements are being obtained to provide a consistent
description of the regrowth mechanisms and to assess the
potential of laser-annealed SOS for device applications.
If it is determined that laser annealing techniques can
be used to control surface and bulk defect concentrations
in silicon, we will conduct studies of metal-silicon
reactions on defect-controlled silicon prepared by laser
processing.

In additional experiments, we conducted ecperiments
with Stanford University in support of another ARO-funded
program (DAAG-29-78-G-0119) on CW-laser-assisted diffusion
and activation of Sn in GaAs from a SnO_2/SiO_2 source.
These experiments have a direct relationship to our study
of metal-semiconductor reactions and gave us the opportu-
nity to investigate another metal-semiconductor system.
In this report, we will provide a brief description of
experiments conducted in each of these areas.

SUMMARY

Microstructural Defects and Laser-Induced Reordering in SOS

The (100) oriented Si epitaxial layers used in this study were grown by chemical vapor deposition on 3 inch diameter sapphire (Al_2O_3) wafers of (00$\bar{1}$2) orientation prepared by Union Carbide Corporation. Thicknesses of the Si films were in the range, $0.15\,\mu m$ to $0.40\,\mu m$, and the deposition rate was varied between $0.1\mu m$ and $2.4\mu m/min$. Portions of some wafers were implanted at room temperature (RT) with ^{28}Si or ^{31}P ions, with or without a secondary ^{11}B implant. To avoid excessive sample heating during ion implantation, the beam current density was maintained at a level below $1\mu\,A/cm^2$ during all implants.

Laser irradiations were conducted on a scanning CW-laser annealing system and samples exposed to the laser beam from the Si side, using a multimode line ($\lambda = 0.5\mu m$). Beam diameters were $100\,\mu m$ and $140\,\mu m$ and corresponding scan speeds were 5 and 15 cm/sec., respectively, producing a nominal dwell time of $\simeq 1-2$ msec. Uniformly, irradiated areas were obtained by stepping adjacent scan lines by 20 µm. During laser irradiation, substrates were maintained at RT or 300°C using a resistivity-heated vacuum chuck.

Samples were characterized using optical microscopy, scanning electron microscopy (SEM), MeV $^4He^+$ Rutherford backscattering (RBS), channeling, and transmission electron microscopy/diffraction (TEM/TED).

Changes in surface morphology, inidicative of melting and resolidification, occured when the laser power/beam

diameter ratio, P/ϕ, exceeded a threshold value of, $(P/\phi)_m =$ (4-5) $\times$ 10^2 W/cm. At levels of P/ϕ within a window, $(P/\phi)_m$ < $P/\phi \leq$ 1.20 $(P/\phi)_m$, the laser annealed areas were relatively uniform with minimal or no traces of scan lines. At P/ϕ levels >1.20 $(P/\phi)_m$, apparent damage or delamination was observed. The surface uniformity could be improved by additional line scans, although no significant differences could be detected in the channeling spectra for up to 4 repeated line scans. The TEM data also showed no significant alterations or additional improvements in structure after repeated line scans, in agreement with the results from channeling measurements. Areas which had been implanted with Si ions at RT to form a buried amorphous layer were visibly less uniform after laser irradiation than the adjacent control (unimplanted) regions. This is possibly attributed to the higher absorption of the laser light and the lower thermal conductivity of the implanted (amorphous) region. Both channeling measurements and TEM analysis showed no dramatic differences between the implanted and unimplanted regions after laser irradiation. It is interesting to note that the color of the laser irradiated regions (in reflected light) was light yellow, whereas unirradiated regions were darker yellow and implanted (no laser irradiation) areas were dark brown or black.

Rutherford backscattering, channeling energy spectra and detailed angular scans were obtained using a (1-2 mm^2) 1.5 MeV ^{4}He$^+$ beam. The laser annealed SOS structures exhibited a dramatic imrpovement in crystal quality of the epitaxial Si films and the results showed that the films were superior to SOS films of the same thickeness grown or processed by any other technique. As shown in Table 1 and

Figs. 1-4, both the surface channeling yield, X_0, and the average dechanneling rate, d_X/dz, were considerably lower than in the starting CVD material, although still above the values obtianed for a bulk Si crystal of (100) orientation. In addition, the measured full width at half minimum, X1/2, of the angular scans measured for a zone, 500Å below the Si surface was the same in the laser annealed films and (100) bulk silicon ($1.1 \pm 0.1°$). In comparison, the values obtained in CVD (no laser irradiation) films were consistently lower than values for bulk (100) Si by a factor of 10-15%. The results then imply that the laser irradiation improves the crystal quality of the Si layers, both at the surface and at depths into the film.

It can be noted that the crystal quality of thick ($t \simeq 0.4\mu m$) laser irradiated SOS films is improved relative to results obtained for thinner ($t \simeq 0.2\mu m$) films, as shown in Figs. 1 and 2. Films of the same thickness, but of varying initial crystal quality, produced as a result of varying CVD conditions or post-deposition implantation, exhibited essentially the same high crystal quality after laser exposure (within rhe experimental accuracy of the measurement system), as shown in Figs. 2 and 3. The small differences in shape of the aligned spectra measured on the laser irradiated regions do not alter this conclusion. The observed differences could be caused by: 1) presence of a thin oxide layer at the surface, resulting in the respective absence, or presence of a clearly identifiable surface channeling peak, and 2) the presence of residual damage produced by the implantation on the sapphire side of the interface.

To provide further information on the relative changes in crystal quality in terms of microstructural defects

Thickness (µm) of SOS Film		As Deposited		Laser Annealed		Bulk Si <100>	
		X_o	$d\chi/dz$ (μm^{-1})	X_o	$d\chi/dz$ (μm^{-1})	X_o	$d\chi/dz$ (μm^{-1})
0.37		0.13	1.3	0.063	0.2		0.05
0.20	CVD	0.42	1.5	0.16	0.35	0.04	0.04
	(P+B) Implanted	0.77	–				
0.17		0.26	2.1	0.17	0.3		0.04

TABLE 1. Si SURFACE CHANNELING YIELD, X_o, AND AVERAGE DECHANNELING RATE, $d\chi/dz$, FOR 1.5 MeV $^4He^+$ IONS INCIDENT ON (100) SOS FILMS, BEFORE AND AFTER CW Ar LASER ANNEALING IN THE LIQUID PHASE MODE FOR 1 ms. X_o IS MEASURED JUST BELOW THE SURFACE PEAK, OR IN THE ABSENCE OF A PEAK, AT THE POSITION OF THE SURFACE SLOPE CHANGE IN THE SPECTRUM. $d\chi/dz$ IS DEFINED AS THE DIFFERENCE BETWEEN THE INTERFACE AND SURFACE YIELDS, DIVIDED BY THE FILM THICKNESS. SINCE THE EXACT VALUES OF $d\chi/dz$ ARE SENSITIVE TO SURFACE CONTAMINATION AND OTHER EXPERIMENTAL CONDITIONS, THEY ARE GIVEN MAINLY TO SHOW THE GENERAL TREND, RATHER THAN AS VIGOROUS QUANTITATIVE DATA.

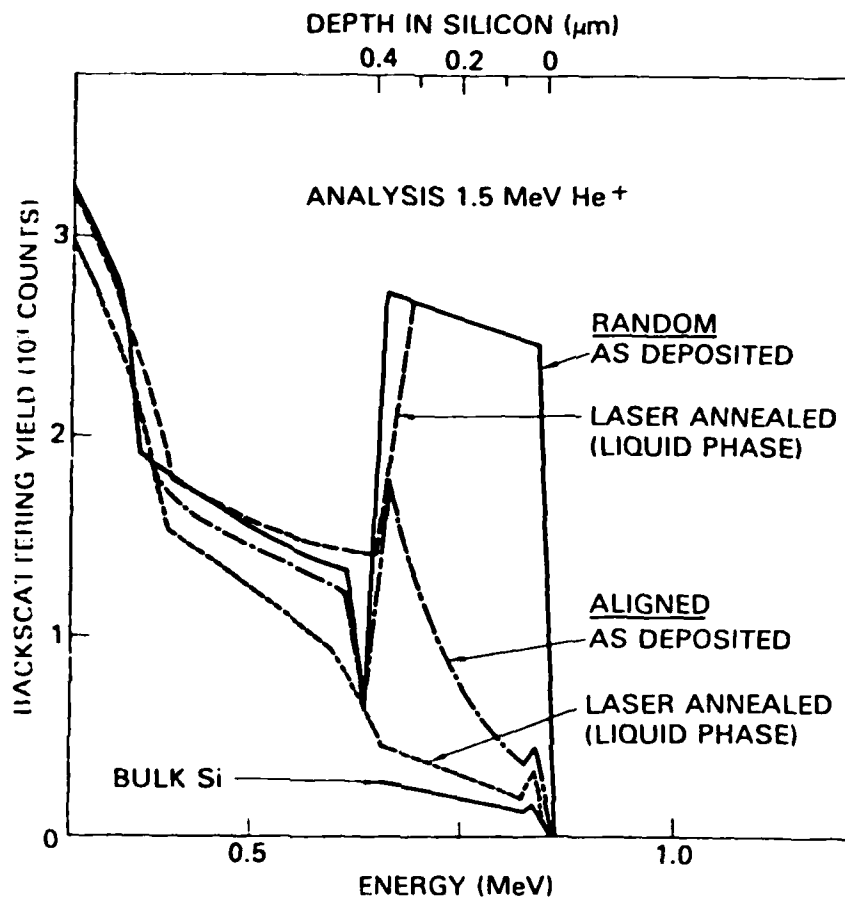## LIQUID-PHASE, CW Ar LASER ANNEALING OF SOS

FIGURE 1. ENERGY SPECTRA OF 1.5 MeV $^{4}He^{+}$ IONS (1-2 mm^{2} SPOT SIZE) BACKSCATTERED AT 170° FROM (100) Si EPITAXIAL FILM OF 0.37μm THICKNESS GROWN ON (01$\bar{1}$2) $Al_{2}O_{3}$ SUBSTRATE. LASER ANNEAL CONDITIONS: BEAM DIAMETER - 140μm; SCAN VELOCITY- 15 cm/sec; SCAN STEP - 20μm; T_{s}= $300^{O}C$; P= 7.5W. ALIGNED SPECTRUM FOR A BULK (100) Si SINGLE CRYSTAL (UNTREATED) IS SHOWN FOR REFERENCE.
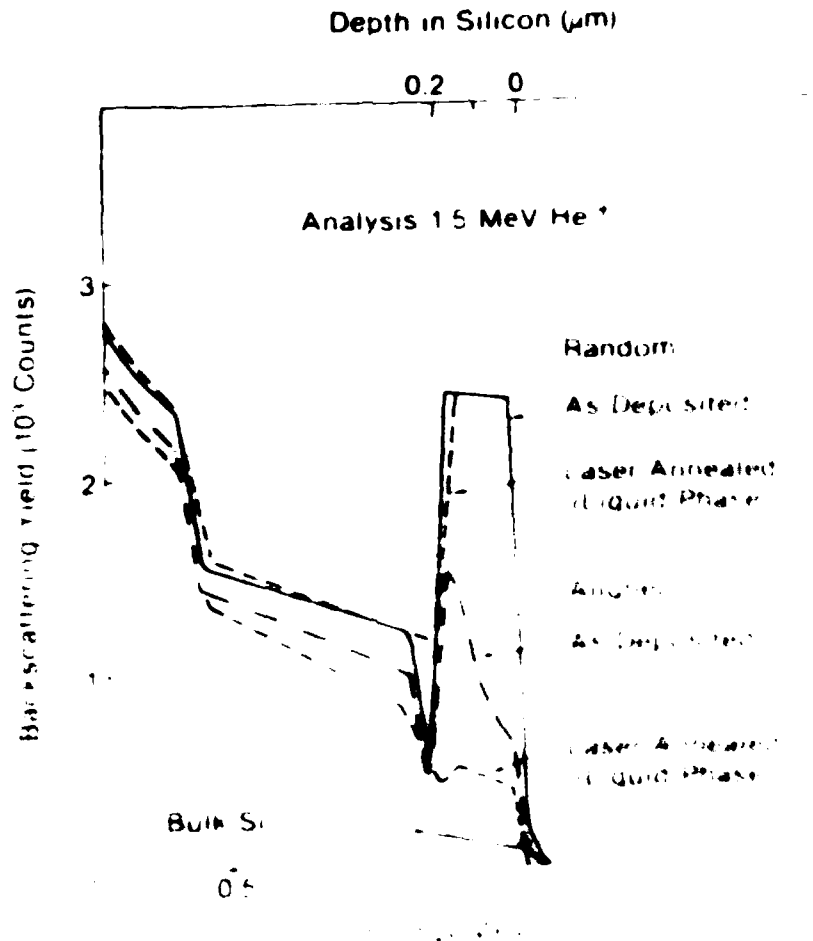
LIQUID PHASE, CW Ar LASER ANNEALING OF SOS

FIGURE 2 ENERGY SPECTRA OF ... ... BEAM DIAMETER 140µm, SCAN ... 20µm, T_s 300°C ... Si SINGLE CRYSTAL IS SHOWN FOR REFERENCE
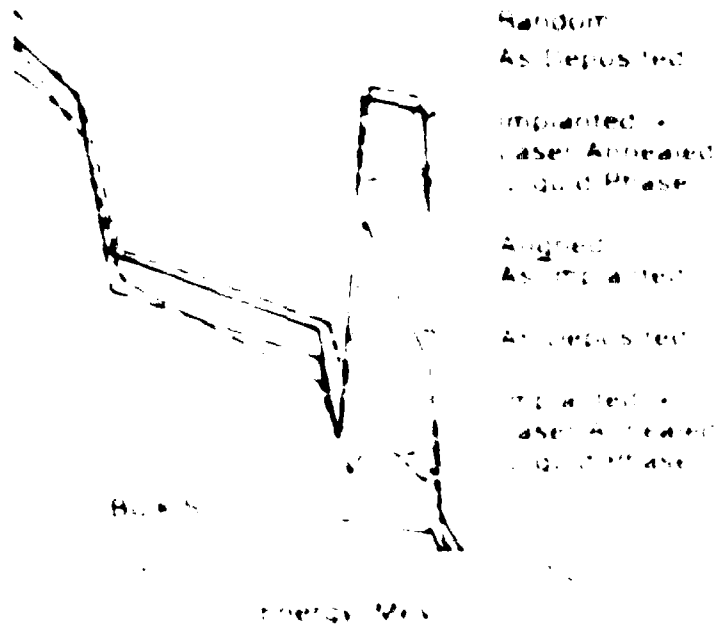
LIQUID PHASE, CW Ar LASER
ANNEALING OF SOS

Depth in Silicon (µm)

0.2   0

- 190 keV 9 x 10¹⁴   P/cm² 7° INC
- 70 keV 1.5 x 10¹⁵   35 keV 7 x 10¹⁴   B/cm² 0° INC

-SOS
At 25°C

Analysis 1.5 MeV He⁺

Random
As Deposited

Implanted +
Laser Annealed
Liquid Phase

Aligned
As Deposited

As Deposited

Implanted +
Laser Annealed
Liquid Phase

Energy (MeV)

ENERGY SPECTRA OF 1.5 MeV ⁴He⁺ IONS BACKSCATTERED FROM 0.20µm THICK Si FILM ON SAPPHIRE AFTER (P + B) IMPLANTATION. THE SIGNAL A BURIED AMORPHOUS LAYER EXTENDING TO THE SAPPHIRE INTER-FACE, BENEATH A ≈500Å THICK SINGLE-CRYSTAL SURFACE LAYER (DOTTED LINE). THE LASER IRRADIATION WAS DONE UNDER THE FOLLOWING CON-DITIONS: BEAM DIAMETER 10µm, SCANNING SPEED 5 cm/s (BIDIRECTIONAL), SCAN STEP 20µm, SUBSTRATE TEMPERATURE 25°C, NOMINAL LASER POWER 5.25W SLIGHTLY ABOVE THE MELTING THRESHOLD). ALIGNED SPECTRA (NOT SHOWN) MEASURED ON AREAS HAVING (i) ONLY THE P IMPLANT AND LASER IRRADIATION AT 5.25W, or (ii) EITHER P OR (P + B) IMPLANTS AND IRRADIATED AT 5.5W WERE SIMILAR TO THE ALIGNED SPECTRUM SHOWN (DASHED LINE, ALIGNED), WHICH WAS MEASURED ON AN AREA IMPLANTED WITH (P + B) AND LASER IRRADIATED AT 5.25W. THE HIGHER BACKSCATTERING YIELD OF THE RANDOM SPECTRUM MEASURED ON THE IMPLANTED AND LASER IRRADIATED AREA (DASHED LINE, RANDOM) COULD BE DUE TO A 3% ERROR IN CHARGE INTEGRATION.

11

present in as deposited and laser annealed films, samples were prepared for TM TED analysis. Specimens were cut into 4mm x 4mm squares and mechanically abraded from the sapphire side to a total thickness of 20-30 μm. Subsequently, samples were subjected to a two stage Ar ion milling to produce thin electron transparent regions. Examination of prepared samples was performed using a Siemens 102 electron microscope at an accelerating voltage of 125 kV. Both bright field and high resolution dark-field imaging modes were used for all analyses.

Representative bright-field transmission electron micrographs obtained on as deposited and laser annealed samples are shown in Figs. 4 and 5, for 0.37μm and 0.17μm thick Si films, respectively. In the as-deposited films, a large density of stacking faults, twinning zones, and dislocation zones are typically observed, producing large, laterally variable regions of disorder in the films. In all cases, the average density of defects within films was consistently high. In contrast, after laser annealing, a substantial reduction in defect density is observed throughout the film thickness. Regions as large as 25 μm x 25μm in the laser irradiated regions were found to be defect-free with only an occasional line defect observed in other laser irradiated areas. Consistent with the channeling data, we observed that the thicker films displayed a smaller number of randomly nucleated defects than the thin films. In all cases, it is of significance to note that the presence of prominent twinning observed by TED in the as-deposited films is <u>not</u> detected in the laser irradiated films.

Comparison of both multiply (laser) scanned and laser irradiated ion-implanted films show no significant differences or alterations in cyrstal to the results obtained
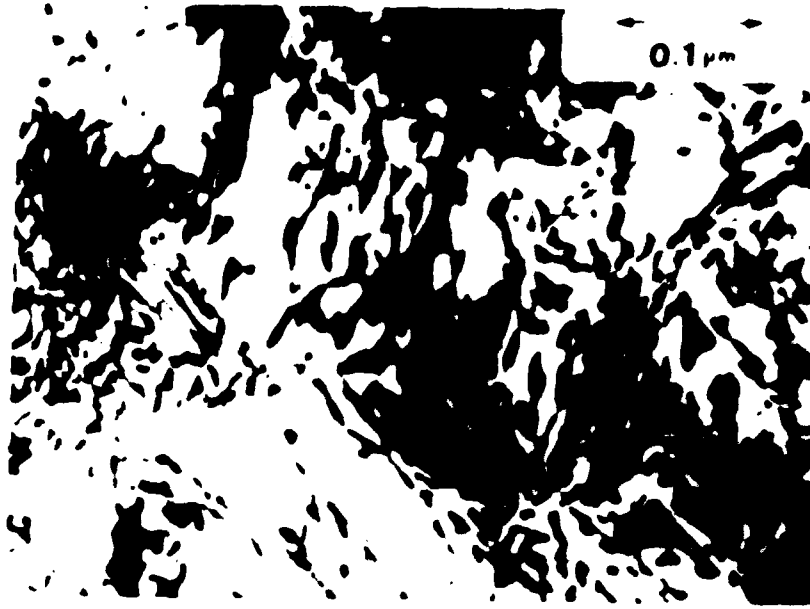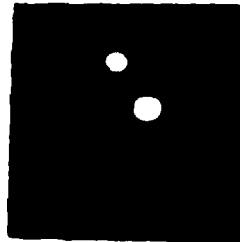
12

As Deposited

Laser Annealed

0.1 μm

0.1 μm

FIGURE 4. PLAN VIEW TRANSMISSION ELECTRON MICROGRAPHS OBTAINED ON AS-DEPOSITED (CVD) AND LASER IRRADIATED SOS FILMS (t_{si} = 0.37 μm) CORRESPONDING TO SAMPLE IN FIG. 1.

As Deposited

Laser
Annealed

0.1 μm

FIGURE 5.   PLAN VIEW TRANSMISSION ELECTRON MICROGRAPHS
OBTAINED ON AS-DEPOSITED (CVD) AND LASER
IRRADIATED SOS FILMS (t_{s1}= 0.17 μm) CORRESPONDING
TO SAMPLE IN FIG. 2.

after a single laser scan of CVD or ion implanted samples. In each case, we observe large regions of defect-free Si and a dramatic change in crystal quality relative to the as-deposited films. Multiple laser scans do not either introduce additional defects or further improve the crystal quality obtained after a single laser (melt-mode) recrystallization consistent with the data obtained from RBS and channeling measurements.

The results obtained in these experiments indicate that the regrowth mechanism induced by the laser irradiation involves: 1) complete melting of the Si film and 2) subsequent epitaxial regrowth starting at the $Si-Al_2O_3$ interface. From the data obtained, epitaxial regrowth initiation from the surface of the Si film is neither warranted nor expected. The surface morphology of the films after the use of a thin transparent encapsulating layer deposited on top of the Si layer and by increasing the laser beam aspect ratio.

Laser Assisted Diffusion and Activation of Tin
from a SnO2/SiO2 Source

In cooperative experiments with Stanford University,
we have investigated the metallurgical modifications
induced after thermal and scanning laser annealing treat-
ments of spin-on SnO_2/SiO_2 layers on GaAs substrates.

Semi-insulating, Cr-doped GaAs substrates of (100)
orientation were coated with a double "source cap" layer
consisting of a 0.3 μm spin-on SnO_2/SiO_2 film covered
by a 0.5 μm CVD-SiO_2 film. To prevent delamination of the
double layer source-cap during laser irradiation, a slow
thermal ramp was carried out in a flowing N_2 environment.
Typical thermal pre-treatment for optimum results consists
of a ramp from room temperature to 900°C in 15 minutes.
This step breaks down the barrier introduced by a native
oxide layer, produces initial intermixing and allows the
diffusion process to proceed.

Following thermal ramping, samples were subjected to
scanning CW-Ar laser annealing using a beam spot diameter
of 50 μm, a scan velocity of 12 cm/sec and a scan step
spacing of 15 μm between lines. To reduce thermal stress,
the substrate was maintained at a temperature of 350°C
during laser irradiation. Using calculations and curves
of laser induced temperature in GaAs, the maximum surface
temperature was obtained for each laser power level used
in the experiments.

The diffusion of tin was first studied in a regime
where the laser power was kept below the level required
to melt the substrate. The laser power for this condition
was determined by observing the laser power required to

16

just produce visible thermal etching and then reducing the settings by 5%. A power level of $P = 0.61W$, leading to a maximum induced temperature of about 800°C, was obtained. A series of 1, 3 and 5 scan frames were performed with the double layer "source-cap" remaining on the substrate. A Van der Pauw Technique was used to characterize the resulting sheet resistivity, Hall mobility and sheet carrier concentration. The results are summarized in Table 2. The increase of the sheet carrier concentration from 2.44 to 3.01×10^{13} cm^{-2}, accompanied by a decrease of sheet resistivity with a larger number of scans, illustrates the diffusion process.

SIMS analysis was performed on a sample thermally ramped only and on a sample scanned 5 times after the ramping. The profiles show ans increase in Sn concentration and an in-diffusion of about 150 Å. To investigate the contribution of the irradiation to the diffusion form the source-cap, compared to the activation of the impurity sitting in the substrate after the ramp, the source was removed before the laser scans. The reflectivity of the bare substrate (after the thermal ramp) was measured and the incident laser power adjusted to reach the same maximum temperature ($\simeq$ 800°C) as before. The wafer was scanned five times and the sheet electrical measurements presented in Table 2 were carried out. The results, when compared with those obtained with the "source-cap" on, suggest that the total increase in active impurities due to laser irradiation is 77% from the source and 23% from the activation of Sn introduced during the ramp.

The action of the laser is found to be more significant if the sample is left "at temperature" for a short time after the ramp. For this reason, the above experiment was repeated

TABLE 2

Sheet Electrical Measurement of the Sn Diffused Layer
Induced by Repetitive Laser Scans

	$\rho (\Omega / \square)$	$\mu_H (cm^2/V.sec)$	$N_{s (cm^{-2})}$
Thermal Ramp to 900°C in 15 Min.	122	2098	2.44×10^{13}
1 Scan with "Source Cap"	118	2017	2.63×10^{13}
3 Scans with "Source Cap"	117	1838	2.91×10^{13}
5 Scans with "Source Cap"	107	1940	3.01×10^{13}
5 Scans with NO "Source Cap"	118	2057	2.57×10^{13}

after thermally ramping the substrate and its source to 900°C
and leaving it for 5 minutes longer at 900°C. A series of 5
scans inducing a maximum temperature of about 800°C was then
performed. A differential van der Pauw technique was used to
profile these samples. Figure 6 shows the results obtained
before and after irradiation. A net increase in carrier con-
centration to a value of about 8×10^{-3} is observed after
the scans. The total Sn profile was also obtained using a
Rutherford backscattering system. A 2.2 MeV incident helium
beam incident on the GaAs substrate was used after removal of
the source. A sample having received a thermal treatment
only, another one receiving additional laser scans leading
to $T_{max} \approx 800°C$, and a third one scanned at higher laser
power leading to $T_{max} \approx 850°C$, were analyzed. The Sn profile
is characterized by a large peak concentration at the surface
which increased after laser scan, probably showing Sn dif-
fusing from the source.

Both the R.B.S. profiles and those obtained using SIMS
analysis show an anomalously high concentration of Sn close
to the surface. This suggests that a chemical reaction takes
place in addition to the diffusion process. To study this
possibility, a sample ramped to 900°C and a sample ramped and
scanned 5 times at a power inducing a temperature of 800°C,
were prepared for T.E.M. and diffraction analysis using con-
ventional jet thinning techniques. Bright-field (Fig. 7)
and dark-field transmission electron micrographs indicated
precipitation after thermal ramp and after laser processing.
Selected area electron diffraction patterns revealed that
the precipitates were composed of a tin arsenic compound:
Sn_3As_2. Additionally, an amorphous $\beta-Ga_2O_3$ was detected in
the samples. After laser irradiation, we observed an increase
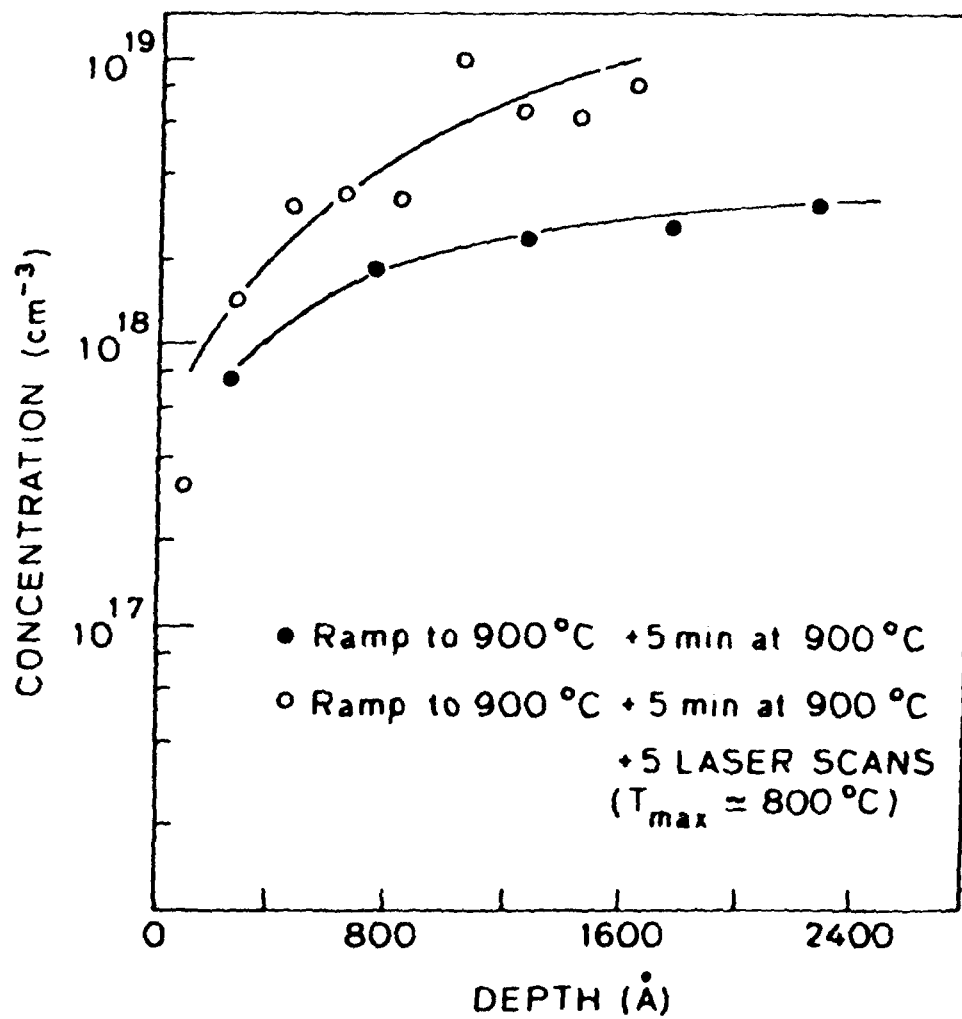of the amount of surface coverage by $\beta-Ga_2O_3$ crystallites.

19

FIGURE 6. ELECTRICAL PROFILES FOR Sn OBTAINED USING A
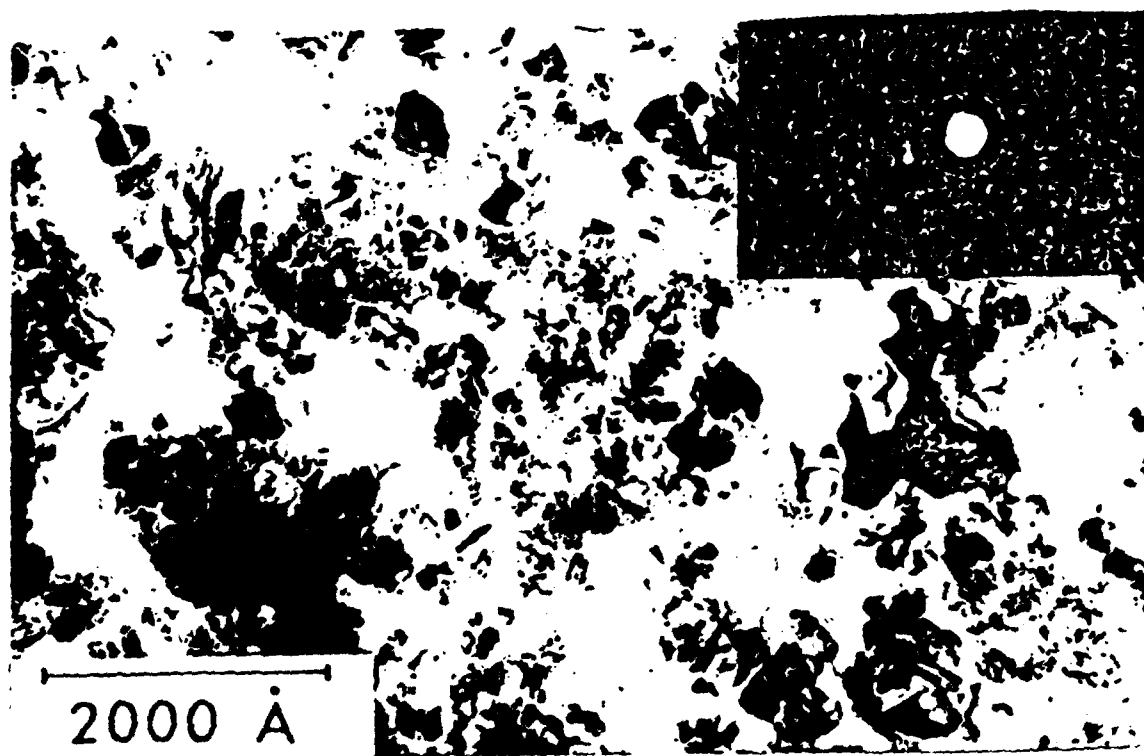DIFFERENTIAL VAN DER PAUW TECHNIQUE.

FIGURE 7. BRIGHT-FIELD TRANSMISSION ELECTRON MICROGRAPH SHOWING FORMATION OF As_2Sn_3 PLOTS. IN THE UPPER RIGHT HAND CORNER ARE THE RINGS ASSOCIATED WITH βGa_2O_3 AND As_2Sn_3. THE d VALUES WERE MEASURED AND CHECKED TO BE CONSISTENT WITH ABOVE COMPOUNDS.

In all cases, the surface oxide film appeared as a laterally discontinuous film.

From the results obtained it has been shown that CW-scanning laser annealing can assist in the diffusion and activation of Sn in GaAs. The observed increase in Sn concentration and the subsequent substantial increase in Sn_3As_2 precipitates after thermal ramping and laser annealing show that a simple "doping" model cannot alone explain the effective formation of the n^+ layer and that the alloy formation is correlated with the observed activity. In either case, the technique described appears attractive for GaAs contact technology.

END

DATE
FILMED

11-81

DTIC